Assessing the Feasibility of Achieving Functional Recovery Goals through Seismic Retrofit of Existing Reinforced Concrete Buildings

Negar Mohammadgholibeyki[1a], Maria Jose Echeverria[1b,c], Amir Safiey [d], Dustin Cook[e], Maria Koliou[a], and Abbie B. Liel[b]

Damage from past earthquakes has significantly hampered post-earthquake building function, threatening community resilience, and motivating consideration of functional recovery in building design and assessment. This study examines whether it is feasible to achieve functional recovery in retrofit of existing reinforced concrete buildings, focusing on seven buildings retrofit with various motivations and strategies. The seismic response of these buildings was nonlinearly simulated, and functional recovery was probabilistically assessed. The results show that retrofits targeting life safety may or may not achieve functional recovery goals. Achieving functional recovery depends especially on the reduction of drift demands and collapse probability. However, the acceleration increase associated with many retrofits can increase function loss due to the criticality of acceleration-sensitive nonstructural components if such components are not retrofitted. We also examine other performance metrics, i.e., economic losses and immediate occupancy limits of ASCE/SEI 41, showing that these provide imprecise, and in the case of the immediate occupancy conservative, proxies for functional recovery.

INTRODUCTION

Past major earthquakes, such as those in Northridge, California, and Christchurch, New Zealand, have underscored the significant impacts of earthquake damage to buildings on community resilience (Alesch et al., 1998; Stevenson et al., 2011). Among such examples, after

[1] Mohammadgholibeyki and Echeverria are co-first authors and contributed equally to this work.

[a] Zachry Dept. of Civil and Environmental Engineering, Texas A&M University, College Station, TX, 77843, US
[b] Dept. of Civil and Architectural Engineering, University of Colorado Boulder, Boulder, CO, 80309, US
[c] Dept. of Structural and Geotechnical Engineering, Pontificia Universidad Católica de Chile, Santiago, Chile
[d] Dept. of Civil and Environmental Engineering, Auburn University, Auburn, AL, 36849, US
[e] National Institute of Standards and Technology, 100 Bureau Drive, Gaithersburg, MD, 20899, US

the Northridge earthquake, the Chatsworth Post Office was closed for 19 months due to structural damage, which interrupted the community's mail service (Collins, 1995). In Christchurch, while some of the hospitals reopened relatively quickly, Christchurch Hospital had a significant loss of function for several days following the earthquake (including closure of the inpatient wards for 14 days, surgical and obstetrics-gynecology for 30 days, and support services for 30 days) (Jacques et al., 2014). In hospitals, this loss of function is due, in significant part, to damage to nonstructural components (Yavari et al., 2010; Jacques et al., 2014). Taken together, the assessment of repercussions after such earthquake events has demonstrated that the current seismic design, as well as retrofit codes and guidelines, generally meet their life safety goals (ASCE/SEI, 2016). However, they do not necessarily lay the conditions for timely or orderly post-earthquake recovery, which is essential for achieving community resilience goals (Porter, 2016).

Building reoccupancy and functional recovery are earthquake recovery-based objectives or post-earthquake performance states (Bonowitz, 2011; Cook et al., 2022) that can be measured in units of time. These objectives can be used to link decisions about the design and retrofit of individual buildings to recovery time and, thus, to community resilience goals. Reoccupancy is a performance state in which a building is safe for shelter and entry/egress. Functional recovery is a performance state in which a building can support basic intended functions associated with pre-earthquake building occupancy (NIST/FEMA, 2021). A third performance state, full repair, refers to a performance state in which a building is fully restored to its pre-earthquake condition (Cook et al., 2022), but this state is not our focus here. Functional recovery is a challenging performance state because it requires the implicit or explicit definition of what is required for building function, which is understood to be something less than full pre-earthquake functionality, but more than the minimum required for reoccupancy (NIST/FEMA, 2021). For example, a hospital may be functional but with a reduced capacity, and, thus, longer patient waiting times (Cimellaro and Piqué, 2016). Several building-specific factors affecting the definition of basic function and functional recovery have been identified in the literature, including building use, occupancy, the criticality of function, and user adaptations (Buckalew et al., 2020; California Legislature, 2021; NIST/FEMA, 2021; Li et al., 2022; Zhan et al., 2022; EERI, 2019; Molina Hutt et al., 2022a; Davidson et al., 2022). NIST/FEMA (2021) also identified community factors, such as socioeconomic characteristics, that affect the definition of functional recovery.

Due to the growing interest in quantifying, utilizing, and codifying functional recovery, several frameworks have been proposed to operationalize this concept. An early example was the Resilience-based Earthquake Design Initiative for the Next Generation of Buildings (REDi), introduced by Almufti and Willford (2013), which quantifies reoccupancy and recovery time as a post-processor of FEMA P-58 probabilistic seismic performance assessments (FEMA, 2018). REDi uses repair classes to identify component damage states blocking function and estimates their repair times to determine time to return to function. To address limitations in the repair class idea and REDi's implementation as a post-processor, as well as conservatisms in a repair schedule that completes all structural repairs before nonstructural, more recently, Terzic and Villanueva (2021), Molina Hutt et al. (2022b) and Cook et al. (2022) proposed probabilistic frameworks for calculating the functional recovery time of buildings. These frameworks adopt various sets of assumptions, detailed below, to explicitly relate building component damage, as determined from probabilistic seismic performance assessment, to operation of key building systems to functionality. The Cook et al. (2022) framework has been advanced by the FEMA-funded ATC 138 project for incorporation into the FEMA P-58 methodology (ATC, 2021).

Terzic et al. (2021) modeled building function as compromised when the fraction of damaged components is larger than a preset damage threshold, as defined for the distinct states of partial and full function losses. Cook et al. (2022) defined building function at the tenant unit level in terms of building systems performance (e.g., performance of building envelope, elevators, etc.), linking component damage to building system operation to function through fault trees. Molina Hutt et al. (2022b) considered multiple recovery-based objectives and adapted the repair class concept from REDi to identify the required building repairs for achieving the desired recovery state. All of these methods consider both the time required to repair post-earthquake damage and the "impeding factors," such as inspection and contractor mobilization, etc., that delay the start of repairs. Cook et al. (2022) defined impeding factors' delays based on conditions associated with each factor. For instance, the financing trigger is reached if the owner's cash on hand is less than the estimated repair costs. Molina Hutt et al. (2022b) defined impeding factor delays that are a function of the maximum repair class of a building. Terzic and Villanueva (2021) called the impeding factors "mobilization activities and delays" and related them to the limit state of the building (no loss, partial loss, and full loss) determined by subsystems' and systems' fault trees.

In parallel to this framework definition, several studies have also assessed the functional recovery of different buildings as illustrative examples using the available probabilistic frameworks. Paul et al. (2018) applied the REDi approach to a university campus in British Columbia (Canada), which includes 328 low-rise light wood frames and low to mid-rise reinforced concrete (RC) wall buildings, to assess the post-earthquake recovery time. They quantified the number of students displaced from campus housing over time for probable and rare return period ground shaking as one of the consequences of lack of function. Cook (2021) applied the Cook et al. (2022) framework to the Imperial County Services Building, a real 6-story RC frame-wall building that was in fact demolished after the 1979 Imperial County earthquake. Looking at the building's performance over a range of intensities, that study concluded that the functional recovery performance of this older non-ductile building was highly impacted by the structural damage, particularly the severe structural damage at the first story that indeed resulted in red-tagging of the building.

Terzic and Kolozvari (2022) evaluated the functional recovery of a 42-story RC-core wall residential building using the Terzic et al. (2021) framework, assuming that the threshold for loss of function was severe damage to 5 % of any relevant class of nonstructural components. They concluded that nonstructural components did not significantly impact the functional recovery time, and structural damage, rather than nonstructural components, mainly governed the functional recovery time The median recovery time at the 475-year return period was reported as 250 days. Molina Hutt et al. (2022a) examined the functional recovery of tall buildings by two archetype examples (42- and 40-story) located in San Francisco, California. At the 475-year return period, the median downtime to functional recovery was obtained as 222 and 169 days for the 42- and 40-story buildings, respectively, assuming site class D and baseline recovery planning. As the structural system damage governed the recovery times, the authors explored the possible reduction of long downtimes by examining more stringent drift limits in design. Taghvaei (2022) also applied the framework proposed by Molina Hutt et al. (2022b) to a 30-story RC wall building in Vancouver, Canada reporting median functional recovery time of 255 days at the 475-year return period); that study found that the main contributor to functional recovery for the considered wall building was the slab-column connection damage.

Cook and Sattar (2022a) preliminarily benchmarked code-conforming buildings' performance by assessing a set of modern RC buildings using the Cook et al. (2022) method. In addition, they redesigned the special moment frames with different design base shear requirements, seismic importance factors, and drift limits. They indicated that the more aggressive structural design requirements and further design considerations to mitigate nonstructural components' damage could significantly reduce the functional recovery time. For example, they indicated that the expected functional recovery times for the baseline archetypes (4- and 12-story buildings) were around 160 to 200 days for the design earthquake, while with the improvements in design parameters, these times were reduced to 100 to 110 days. Subsequently, Cook and Sattar (2022b) performed a sensitivity analysis on the fragility parameters of various nonstructural components for 20 simplified building models representing RC frame and cantilever wall systems to evaluate the effects of nonstructural damage on buildings' functional recovery (using again the Cook et al. 2022 method). They recommended more in-depth research on piping components, the highest contributors of nonstructural components in the functional recovery time in their assessments. Overall, the importance of the nonstructural components relative to structural performance depends on the definition of function and the overall structural seismic performance.

Research efforts to date have focused on developing probabilistic frameworks for quantifying functional recovery, exercising these for different buildings to explore influential factors for functional recovery. The goal of such research has been to inform the achievement of recovery-based objectives in new buildings – what Haselton et al. (2020) refer to as "functional recovery design." In contrast, there have been limited studies on the potential of retrofitting existing buildings to achieve functional recovery goals, even though the existing building stock is expected to contribute significantly to earthquake damage and recovery consequences.

Among existing buildings, the retrofit of non-ductile RC buildings is of particular interest because of the large number of such structures in seismic prone regions (e.g., an estimated 20,000 pre-1980 non-ductile RC buildings in California) and their significant seismic vulnerabilities. The Christchurch Earthquake demonstrated the impacts on communities with substantial numbers of such buildings not yet retrofitted (Kim et al., 2017). Accordingly, several local jurisdictions in the U.S. have mandated, planned to mandate, or considered the seismic evaluation or retrofit of such buildings to address life safety and enhance resilience (SEAOSC, 2016). Thus, a growing number of seismic retrofit projects of RC buildings can be expected in coming years, motivated by life safety, and an understanding of the technical solutions that enable engineers to achieve functional recovery goals is essential for reaching community resilience goals.

The American standard for the seismic evaluation and retrofit of existing buildings, ASCE/SEI

41, defines seismic performance levels as immediate occupancy (IO), life safety, and collapse prevention (ASCE/SEI, 2017). A building fails to meet the performance level if a single component exceeds the threshold associated with the performance level; such criteria are defined based on the structural responses of the building, e.g., plastic hinge or chord rotations. The IO state corresponds to "a post-earthquake state in which a building remains safe to occupy and essentially retains its pre-earthquake condition" (ASCE/SEI, 2017). Despite being defined similarly, functional recovery and IO may not have an explicit correlation in terms of global structural performance since IO is evaluated at a component scale (Cook and Liel, 2021).

There are some similar key challenges in achieving functional recovery goals for both new buildings' design and retrofit of existing buildings. Designing for recovery-based objectives requires enhanced seismic design, which may increase the construction cost compared to current practice (NIST/FEMA, 2021). Thus, the main concern is financial costs (real and perceived), and the owners' hesitation to invest in achieving recovery-based objectives. Moreover, there are several challenges beyond the cost. For example, there is a lack of guidance on how to achieve functional recovery including, for example, uncertainty in design of nonstructural components and lack of clarity on the critical seismic hazard levels and key metrics. There is also an inherent contradiction between community-scale goals for resilience and what can practically be accomplished in design of individual buildings.

However, operationalizing functional recovery goals to retrofit existing buildings is more challenging than new designs. Most retrofit designs focus on targeting life safety by mitigating the specific structural deficiencies identified as critical in the building's vulnerability to collapse. Targeting functional recovery for buildings with significant seismic vulnerabilities may be particularly challenging due to the high cost of life safety retrofits especially for certain kinds of building (Egbelakin et al., 2014; Zhang et al., 2022). There is also potentially a shorter time horizon from the remaining building lifespan to benefit from these investments. NIST/FEMA (2021) recommends considering alternative and lower criteria for existing buildings' retrofit relative to new buildings' design, resulting in defining different target recovery times for retrofit, which may depend on the criticality of building function in a community. Additionally, communicating what owners gain beyond code compliance and life safety with functional recovery and the timeline of these gains is challenging (Echeverria et al., 2023). Another difficulty is that, for many retrofit projects, owners require a design that reduces disruption for occupants (Echeverria et al., 2023).

SCOPE

This study aims to fill the gap in the literature by investigating the feasibility of retrofitting existing RC buildings with various characteristics to meet recovery-based objectives. We gathered information from seven older existing RC buildings with different lateral resisting systems, including the wall, frame-wall, and frame buildings, retrofitted with various strategies, including walls, dampers, and fiber reinforced polymers. We then performed nonlinear simulations and collapse assessments of each building's model and input those results to perform FEMA P-58 vulnerability and functional recovery assessments based on Cook et al. (2022) and ATC (2021). Finally, we compared the functional recovery assessment results of existing and retrofitted buildings. Primarily, we discuss the impact of each retrofit strategy on the structural responses, the functional recovery time results, and the effects of improving retrofitted buildings' nonstructural components on functional recovery times. The findings of this study aim to assist engineers and policymakers in evaluating the feasibility of achieving functional recovery goals for future retrofit projects and in consideration of such in codes and standards.

METHODS FOR ASSESSING FUNCTIONAL RECOVERY IN RETROFIT

Figure 1 presents an overview of our study, showing how the functional recovery assessment is integrated with the FEMA P-58 (2012; 2018) methodology, and applied to existing RC buildings. Our study consists of the following steps: selection of existing buildings, development of nonlinear simulation models, ground motion selection and scaling, structural analysis through nonlinear dynamic analyses, loss and functional recovery assessment, and comparison of the results of existing (unretrofitted) and retrofitted buildings in terms of expected annualized losses and recovery times, and median recovery times for reoccupancy and functional recovery. These steps are described in more detail below.

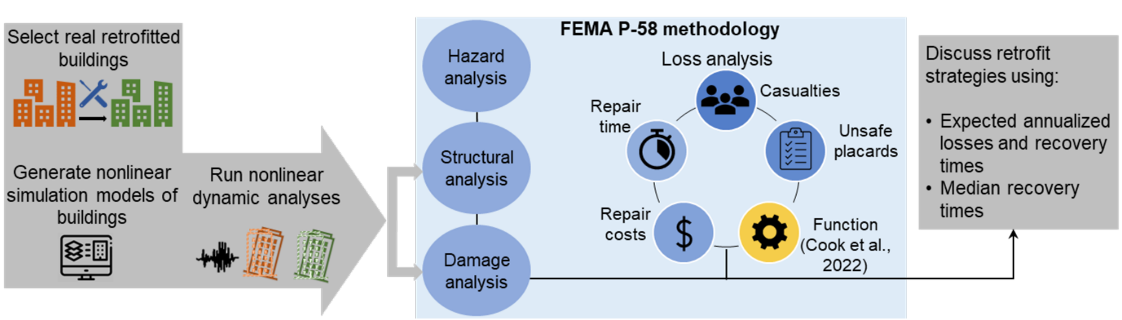

Figure 1. Overview of the study, showing how functional recovery assessments are used to assess the feasibility of retrofit to achieve these goals.

SELECTED BUILDINGS

In this study, seven existing buildings were selected, representing older non-ductile RC buildings with wall, frame-wall, and frame lateral force resisting systems, as summarized in Table 1. These buildings were selected based on the availability of: (1) building drawings providing the information needed to create structural analysis models, (2) documentation of structural deficiencies, and (3) documentation of structural (and nonstructural, when available) retrofit strategies employed. Information from real buildings and retrofit solutions was a starting point for modeling the selected buildings and for exploring the structural and nonstructural components' upgrades. However, we pursued some alterations of design details, both to simplify complex geometries not impacting the overall assessment and to de-identify the buildings. We also assumed upgrades of nonstructural components, even when information on this was not available, as described in more detail below. We focused on buildings located in the U.S. or similar to U.S. construction. The two RC wall buildings (W1, W2) have structural deficiencies mainly related to the presence of vertical irregularities, particularly flag shape walls and vertically discontinuous walls. The frame-wall building (FW3) has structural deficiencies associated with low strength of materials and torsional irregularity. Four RC frame buildings were also considered (F4 to F7), characterized by structural deficiencies such as soft story, limited deformation capacity, and strong-beam/weak-column in some locations.

These buildings were retrofitted using various retrofit strategies (e.g., adding new walls, dampers, and fiber reinforced polymers). Although this information was not always available, most of the retrofits were voluntary and intended to improve life safety and asset protection. In other cases, the retrofit was motivated by earthquake damage or by an insurer. None of the retrofits were governed by California jurisdictions' recent mandatory retrofit ordinances.

MODELING APPROACHES

A nonlinear simulation model was developed for each case study building to perform dynamic analyses. As shown in Table 2, the simulations differ regarding the analytical model configuration, i.e., 2D or 3D models, and the analysis software. In all cases, the models were developed to capture the critical modes of strength and stiffness degradation as they influence earthquake responses and damage. However, various approaches were used to capture building-specific component and system responses and avoid limiting the assessment performed in this study to a specific software and modeling paradigm. Where 2D models were used, these represented the expected critical direction. The critical structural components, which were beams, columns, and walls, were in some cases modeled with a concentrated plasticity approach and in some cases with fiber or finite elements, as needed to represent the expected failure modes. The concentrated plasticity approach captures hysteretic flexural behavior, including deterioration, through the modified Ibarra-Medina-Krawinkler (IMK) model (Ibarra et al., 2005).

Fiber sections were used for flexural-governed components based on Kent-Scott- Park concrete and Giuffré-Menegotto-Pinto steel constitutive models (Kent and Park, 1971; Menegotto, 1973; Filippou et al., 1983). Finite elements employed the Parabolic model (Feenstra, 1993) for compressive behavior and the Hordijk and Reinhardt (1993) model for tensile behavior of concrete and both include a fracture energy-based regularization. The reinforcing steel was modeled using the Giuffré-Menegotto-Pinto model.

For gravitational loads, the (unfactored) dead load plus 25 % of the design live load was considered as the expected load, and also applied as seismic mass (ASCE/SEI, 2016). The effects of viscous damping were considered using the Rayleigh damping formulation with an equivalent viscous damping ratio in the range of 2 % to 5 % over the range of elastic periods from 0.2T to 1.5T (where T is the elastic fundamental period) (Deierlein et al., 2010). Reasonable periods and damping ratios needed for the definition of the Rayleigh model were considered depending on the building and its sources of energy dissipation. To simplify the modeling process, soil-structure interaction effects were excluded, and models were fixed at the base, except in buildings FW3 and F7, where column bases were pinned because footings lacked significant moment-resisting capacity. For all models, in-plane rigid diaphragms were assumed, and effective component stiffness values were adopted from the Tall Building Initiatives recommendations (TBI, 2017). In most cases, we did not explicitly model joints, except where the expected capacity of the joints was lower than the maximum demands from the columns and beams framing into the joint. In these cases, joints were modeled following the recommendations of ASCE/SEI 41-17 Section 10 (ASCE/SEI, 2017). We validated building models by comparing the modal, and structural responses, if possible, with those reported in past studies and reports, e.g., (Echeverria et al., 2022; PEER, 2005; NIST, 2022; Miyamoto et al., 2017; Miano et al., 2019), in some cases, the results to which we compared to are unpublished.

Table 1. Main characteristics of the selected case study buildings

Building ID	Structural System	Year Built	Occupancy	# of Stories	Location	Structural deficiencies	Retrofit motivations & performance target[b]	Structural retrofit strategies
W1[a]	Cantilever Shear Wall	2000s	Multi-Unit Residential	20	Chile (Assumed Southern California)	Thin unconfined walls subjected to high axial loads	Post-earthquake repairs and strengthening with a target performance of Collapse Prevention for seismic hazard similar to BSE-2E	Adding special boundary elements and increasing wall thickness.
W2	Cantilever Shear Wall	1950s	Commercial Office	4	Pacific Northwest	Vertical irregularity due to discontinuity of the sole transverse shear wall	Voluntary at owner's request with a target performance of Life Safety and Collapse Prevention for seismic hazard similar to BSE-1E and BSE-2E, respectively.	Adding transverse RC walls at each of the buildings' ends, FRP on columns at the end of the discontinuous RC wall
FW3	Frame-wall	1910s	Commercial Office	5	Southern California	Low original design material strength for concrete and reinforcement, high torsion due to the presence of a shear wall at the north side of the building	Voluntary at owner's request to preserve the historic character of the building while complying a target performance of Life Safety for seismic hazard similar to BSE-1E	Strengthening of perimeter perforated shear walls in the E.W. direction with piers and spandrels, strengthening of perimeter column foundations.
F4	Existing: Frame Retrofitted: Frame-wall	1960s	Education Office	3	Northern California	Soft story, strong-beam/weak-column in some locations	Voluntary at owner's request with a target performance of Life Safety for seismic hazard similar to BSE-2E	Adding a RC wall in each building's direction.
F5	Existing: Frame Retrofitted: Frame-wall	1960s	Hospitality	7	Southern California	Shear-critical columns with inadequate transverse reinforcement	Retrofit is hypothetical with a target performance of Life Safety and Collapse Prevention for seismic hazard similar to BSE-1E and BSE-2E, respectively	Adding a RC wall into the frame.
F6	Frame	1970s	Commercial Office	14	Northern California	Soft story at first story, limited deformation capacity, shear-critical beams	Voluntary to increase safety and reduce earthquake insurance premium	Adding viscous dampers at bottommost stories.
F7	Frame	1930s	Multi-Unit Residential	12	Southern California	Lateral force resisting system at first and second stories did not satisfy the design criteria	Voluntary at owner's request to meet Life Safety for seismic hazard similar to BSE-1E	Strengthened transfer beams and diaphragm connections. FRP on perimeter piers. Lengthening of first story shear wall.

[a]This Chilean RC wall building was included in this study because it represents U.S.-like non-ductile wall buildings prior to the 1980s and detailed design and retrofit information was available. This building was assumed to be located in Southern California for assessment.
[b]ASCE/SEI 41-17's seismic hazard: BSE-1E has a 20 % probability of exceedance in 50 years; BSE-2E has a 5 % probability of exceedance in 50 years. In some cases, the performance target was not clearly documented.

Table 2. Summary of modeling approaches for case study buildings

Building ID	Software	Analysis level	Beams	Columns	Walls	Slabs	Others
W1	DIANA	2D finite element model	N/A	N/A	Nonlinear four-node curved shell elements	Linear elastic four-node curved shell elements with effective stiffness	N/A
W2	DIANA	3D finite element model	Linear elastic fully numerically integrated quadratic three-node Class-III Mindlin beam elements		Nonlinear four-node curved shell elements	Linear elastic four-node curved shell elements with effective stiffness	Confined concrete material used to model the additional confinement from the FRP.
FW3	OpenSees	3D Concentrated plasticity	Concentrated plasticity formulation using elastic elements and nonlinear zerolength springs at two ends		Rigid elastic vertical elements with a shear spring in the mid-height	Slabs were not explicitly modeled	Viscous damper material with two node link elements used for dampers
F4	OpenSees	2D Concentrated plasticity	Concentrated plasticity formulation using elastic elements and nonlinear zerolength springs at two ends		Displacement-based beam-column fiber elements-flexural response	Slabs were not explicitly modeled	N/A
F5	OpenSees	3D Concentrated plasticity	Concentrated plasticity formulation using elastic elements and nonlinear zerolength springs at two ends		Displacement-based beam-column fiber elements-flexural response	Slabs were not explicitly modeled	N/A
F6	OpenSees	2D Concentrated plasticity	Concentrated plasticity formulation using elastic elements and nonlinear zerolength springs at two ends		N/A	Slabs were not explicitly modeled	N/A
F7	OpenSees	3D fiber-discretized sections	Force-based fiber beam column element		N/A	Slabs were not explicitly modeled	FRPConfinedConcrete material used for FRPs.

NONLINEAR DYNAMIC ANALYSIS

Nonlinear time history analyses were performed to assess the structural response of each case study building at seven intensity levels. In this study, the FEMA P-695 far-field ground motion set, which is considered to be representative of the seismicity in the Western United States (FEMA, 2009), was used. These ground motions were scaled to seven hazard levels ranging from the 72 to 4275-year return period to represent a range from frequent, service level, to rare, ultimate events. We adopted the spectral acceleration at the fundamental period of each building $Sa(T_1)$ as the ground motion intensity measure (IM). The structural responses were described using global engineering demand parameters (EDPs), namely the peak floor accelerations (PFA), peak story drift ratios (SDR), and residual story drift ratios for frame buildings, and including chord rotations for wall and frame-wall buildings. These EDPs were estimated from the dynamic analysis, except for the residual story drift ratios, which are highly uncertain and sensitive to the modeling assumptions and the ground motion characteristics (Kourehpaz et al., 2021). Hence, we determined the residual story drift ratios using a general inelastic model for residual drift (Cook et al., 2017). EDPs from the 2D models were taken as the same in both orthogonal directions. For excessive residual drifts, i.e., those exceeding 1 %, irreparable damage is assumed so the repair cost is the full replacement cost, and the recovery time is the building replacement time (FEMA, 2018).

The collapse fragilities were described by the lognormal distribution functions (Baker, 2015), using the data from the performed nonlinear dynamic analyses. In some cases, the results from the seven hazard levels were augmented with incremental dynamic analysis to refine the collapse fragility definition with more intensities. For the frame buildings, collapse was defined based on a drift-limit (FEMA, 2013); for the wall buildings, we used a component-based limit (Dabaghi et al., 2019; Abdullah and Wallace, 2021; Echeverria et al., 2022). Numerical instabilities associated with sudden lateral strength and stiffness degradations were also considered to define collapse. To account for modeling and other uncertainties beyond ground motion variability, the lognormal standard deviation of the collapse fragilities was assumed to be 0.6 as per FEMA P-695 (FEMA, 2009). To reflect inconsistencies between the spectral shape of the records used in analysis and the sites' hazard, collapse capacities were adjusted according to FEMA P-695 (FEMA, 2009), using the shape factor (SSF) which depends on the building's fundamental period (T), period-based ductility (μ_T), and the seismic design category.

FUNCTIONAL RECOVERY ASSESSMENT

The functional recovery assessment was performed using the probabilistic method for assessing post-earthquake building performance states of function and reoccupancy proposed by Cook et al. (2022), further developed by ATC (2021) and integrated with the FEMA P-58 methodology, as shown in Figure 1. The FEMA P-58 (2012; 2018) performance-based engineering methodology defines fragility functions for over 700 components and damage states to predict damage states in building components and translate these damage states into performance metrics, such as repair costs and repair times, through associated consequence functions. However, the existing FEMA P-58 methodology estimates only the repair time required to achieve full repair and does not consider intermediate recovery states like reoccupancy and functional recovery. Cook et al. (2022) addressed this limitation by mapping component damage states to systems-level operational performance, and then to building-level performance states, through a series of fault trees. The systems considered are: structural, exterior enclosure, interior components, stairs and elevators, fire suppression, water/plumbing, heating ventilation and air conditioning (HVAC) and electrical/power. Cook et al. (2022) also defined a repair scheduling algorithm and a set of impeding factors that delay the start of repairs. The scope is limited to function effects within the building footprint, and therefore excludes effects from disrupted utility or infrastructure systems. We used the Seismic Performance Prediction Program (SP3) implementation of the functional recovery assessment method (Haselton Baker Risk Group, 2022). The functional recovery assessment takes as inputs: (1) building and seismic hazard characteristics; (2) structural responses, and (3) characteristics of the structural and nonstructural components in the structure.

In this study, the structural and nonstructural components were mapped to the P-58 component libraries based on the building drawings and the information about nonstructural components when available. Due to the lack of information about the retrofit strategies of nonstructural components, we made some assumptions, described in more detail below. In most cases, FEMA P-58 (2012, 2018) structural component fragility functions were considered in this study. However, Echeverria et al. (2022) has shown that FEMA P-58 fragilities are not appropriate for RC walls with critical characteristics like thinness, lack of confinement, high axial loads, or significant vertical irregularities – features that are prevalent in the RC wall buildings examined in this study. Aghababaei et al. (2022) showed how the loss assessments could be over- or under-estimated if the appropriate fragilities are not used. Therefore, for the two RC wall buildings, FEMA P-58 fragilities for RC walls were adjusted by reducing the capacity by 50 % for thin unconfined walls with vertical irregularities, following Echeverria et al. (2022).

The functional recovery assessment also requires defining other assumptions and conditions that influence the factors for repair delays. In this study, we considered a good relationship with the contractor, which presumes that owners have a contractor they know to call, which is common for large institutional owners. We assumed owners have 5 % of the building value available as cash-on-hand available and that the rest of the funding to conduct repairs would be obtained from private loans. We did not account for long lead times to obtain some components, or for regional demand surge. If considered, these factors would increase the total time (Molina Hutt et al. 2022a).

We adopted the default requirements for function of commercial and residential buildings defined in Cook et al. (2022), which require that plumbing and electrical systems are operational, and building envelope and interior spaces are not overly damaged. HVAC systems were assumed to be needed for function. For buildings less than six stories, we considered that the elevators are not needed for function. For buildings with more than six stories, we defined story six as the highest story to which it is acceptable for occupants to access via stairs while the elevators are broken (Molina Hutt et al., 2022b). Where possible, we allowed temporary measures to be taken immediately after the earthquake (before the full permanent repairs are carried out) to mitigate reoccupancy/functionality issues. We also assumed that the buildings' jurisdiction allows for occupancy with a fire watch if the building's fire suppression system is compromised. The replacement times are based on relatively broad assumptions in SP3 Risk Model, and depend on building height, ranging from 400 days (3-story F4) to about 750 days (20-story W1)

Three analyses were performed for each case study building: (1) existing (ex), which considered the original state of design and construction of the building; (2) retrofitted (ret) structural, which included seismic improvements to structural components (summarized in Table 1) and (3) retrofitted structural and nonstructural, which included seismic improvements to structural and nonstructural components. For nonstructural components and systems, in reality, limited upgrades were made. Nevertheless, we optimistically considered possible seismic retrofits that a proactive owner could adopt to reduce the functional recovery time, as described below.

The outcome of the functional recovery assessment is 2500 realizations of recovery times for each of the performance states, at each hazard level of interest. To evaluate the effect of retrofit on losses and functional recovery assessments, we considered the median recovery times at each hazard level as a measure of central tendency. We also calculated the functionality gain associated with retrofit at each hazard level, i.e., the percentage difference between the recovery times of the existing and retrofitted models, using Equation (1),

$$Functionality\ Gain = \frac{T_{ex} - T_{ret}}{T_{ex}} \times 100\ \% \qquad (1)$$

where, T_{ex} and T_{ret} represent the median recovery times of the existing and retrofitted buildings, respectively, at each hazard level. There is significant uncertainty in the assessed functional recovery times, but we do not interrogate these here.

The performance of the existing and retrofitted buildings was also compared in terms of the expected annual losses (EALs) and expected annual recovery times (EATs) for the two recovery performance states: reoccupancy and functional recovery. The recovery time represents the equivalent number of days of function (or reoccupancy) lost annually based on the seismic performance. These values were calculated using Equation (2),

$$E[C] = EAT\ or\ EAL = \int_0^\infty E[C|IM = x]|d\lambda(IM > x)| \tag{2}$$

where, E[C|IM=x] is the expected consequence (where the consequence, *C*, could be economic losses or recovery time) given the IM, and dλ(IM>x) is the derivative of the IM hazard curve (Mitrani-Reiser, 2007).

NONSTRUCTURAL RETROFIT STRATEGIES

Table S1 (supplemental material) summarizes the fragilities from FEMA P-58 (2012; 2018) considered for the existing and upgraded nonstructural components. Retrofit strategies for each group, supported by personal communication with practicing engineers, are briefly described below. In reality, some of the retrofit strategies considered in this study are not very likely, mainly due to the high upgrade costs and lack of guidance for the design, construction, inspection, and maintenance of nonstructural components to achieve functional recovery goals. However, we aimed to consider a reasonable upper limit on the effect of nonstructural retrofit with the assumptions described herein.

<u>Exterior enclosure:</u> We assumed the building surface was glazed (floor to ceiling windows) with the percent of glazing based on the building's occupancy in both existing and retrofit buildings. The type of glazing was upgraded from the insulating glass unit for the existing buildings to monolithic glass (with higher drift capacity) for the retrofitted buildings. Since the use of precast cladding is common for building envelopes in the U.S (WBDG, 2016), we considered it for both the existing and retrofitted buildings.

<u>Interior components</u>: The presence of wall partitions with metal studs, gypsum, and wallpaper was assumed for existing and retrofitted buildings. However, different installations were assumed. For the existing buildings, we considered full height partitions, fixed below with a slip track above, while for the retrofitted buildings, partial height partitions fixed below with lateral bracings above,

which are less susceptible to damage, were assumed. We assumed the existing buildings had suspended ceilings. To reduce this damage and its impacts on function, suspended ceilings were removed in the retrofitted buildings. This practice has recently been seen in post-earthquake repairs (Rodgers et al., 2021). Raised access floors and pendant (non-recessed) lighting were not considered.

Stairs and elevators: For existing buildings, non-monolithic precast concrete stair assembly with concrete stringers and treads without seismic joints was defined, then upgrades on the retrofitted cases consisted of adding seismic joints that accommodate drift. Traction elevators (California prior or post-1976, depending on the building's construction year) were considered in existing buildings, while they were replaced with better performing hydraulic elevators for buildings under 7 stories.

Fire suppression: For existing buildings, we considered fire sprinkler systems with poor/no bracing and non-certified fire sprinkler drops. The certification here refers to California's Office of Statewide Health Planning and Development or OSHPD, (now Department of Health Care Access or Information, HCAI) which certifies hospital design (HCAI, 2022). The retrofit strategies involved replacing the fire sprinkler systems with certified systems, designed bracing, as well as certified fire sprinkler drops.

Water/plumbing: In the existing buildings, we assumed non-certified cold or hot potable threaded steel piping and non-certified cast iron piping with bell-spigot couplings for the potable water piping and the sanitary waste piping, respectively. The seismic upgrades consisted of replacing the buildings' water and sanitary piping with OSHPD-certified piping.

HVAC systems: We assumed that the HVAC cooling/heating equipment was not seismically anchored in the existing buildings, while seismic anchoring to the equipment was added for the retrofitted buildings. We did not consider HVAC exhaust systems.

Electrical/power: We assumed existing buildings have unanchored (not vibration isolated) power distribution panels. Backup battery/generator systems may not be present in multi-story buildings (Terzic and Villanueva, 2021), therefore, building backup systems were not considered. The seismic upgrade replaced the distribution panels with full commercial-grade systems, which include distribution panels, low voltage switchgear, and transformer/primary service.

RETROFIT EFFECTS: RESULTS AND DISCUSSION

This section first discusses the results of the structural analysis in terms of engineering demand parameters, which influence the functional recovery performance assessments, discussed second. The results section concludes with a consideration of whether alternative metrics, such as economic losses or the ASCE/SEI 41 IO limit, may be suitable proxies for functional recovery.

ENGINEERING DEMAND PARAMETERS

Table 3 shows the fundamental elastic periods of the existing and retrofitted building models and their collapse capacities (adjusted for spectral shape). As shown in Table 3, the retrofitted strategies for W1 to F5 have considerably reduced the fundamental period (on average, by 40 %). However, for F6, because the retrofit strategy added only a pair of dampers at the first two stories, there was no significant change in the building's stiffness. Similarly, the retrofit for F7 was relatively minor and local (mainly focused on the first two floors).

Table 3 shows a significant increase in the collapse capacity of buildings with major structural improvements. For example, we observed that the collapse capacity of the retrofitted model of F5 (at the fundamental period of the existing building) increased by 73 % with added structural walls. Improvements in collapse capacities by retrofit in our study were relatively consistent with what has been observed in the literature for ASCE 41-designed retrofits, in terms of both the order of magnitude of the effect and the variation (Harrington and Liel, 2020). (For additional information, Table S9 tabulates the probability of collapse and excessive residual drifts – irreparable damage – per hazard level for the existing and retrofitted models.)

Table 3. Fundamental period and collapse capacities of existing and retrofitted building models

Building ID	# of stories	Fundamental period (sec)		Collapse capacity (g)		
		Existing $T_{1,ex}$	Retrofitted $T_{1,ret}$	Existing $Sa(T_1,ret)$	Retrofitted $Sa(T_1,ret)$	% Improvement
W1	20	0.87	0.75	1.25	1.27	2
W2	4	0.41	0.23	2.21	2.82	28
FW3	5	2.13	1.13	1.27	2.28	80
F4	3	0.87	0.76	1.95	2.18	12
F5	7	1.83	0.55	1.48	2.56	73
F6	14	3.55	3.55	0.15	0.16	7
F7	12	0.77	0.73	1.12	1.07	-4

Figures S1 to S7 (supplemental material) show all buildings' SDRs and PFAs responses. For the buildings with significant upgrades, e.g., W1, W2, FW3, and F5, the SDRs decreased by up to 94 % depending on the building and hazard level, and the PFAs increased by up to 286 %, as expected from the retrofit strategies that resulted in greater stiffness for the retrofitted buildings. In addition, the improvement in the drift response (up to 28 % reduction) of the first two stories of F6 confirms the effectiveness of dampers in dealing with the soft story damage mechanism, with only a relatively small increase in PFAs (up to 40 %) compared to buildings with significant upgrades where they increased drastically (e.g., up to 286 % for FW3). On the other hand, the EDPs did not significantly change for F7, particularly at the higher story levels, because the retrofit was localized. Similarly, the EDPs of F4 did not significantly change because the retrofit was minor, adding a relatively small number of slender walls.

FUNCTIONAL RECOVERY ASSESSMENT

Overview

Figure 2 summarizes the results by presenting the expected (mean) annualized recovery times or EATs for all the buildings. As expected, the times are greater for functional recovery than reoccupancy in all cases, though in the annualized metric these differences are relatively small. These EATs reduced by 1 to 70 % for reoccupancy and 0.3 to 64 % for function with structural retrofit. The buildings with the highest and the lowest percent reductions were F5 and F7, respectively. The combined retrofit of structural and nonstructural components helped to further reduce the EATs in all buildings, providing up to a maximum further reduction of 13 and 41 % for reoccupancy and function, correspondingly. On the basis of the annualized results and the absolute changes in recovery time at key hazard levels, we grouped the buildings into three groups, those with high functionality gain from retrofit: those with moderate gain, and those with small or no gain. These groups are discussed in more detail below.

Effect of structural retrofit

Buildings with high functionality gain

A considerable decrease in recovery times for reoccupancy and functional recovery performance levels was observed for buildings W1 and F5, according to

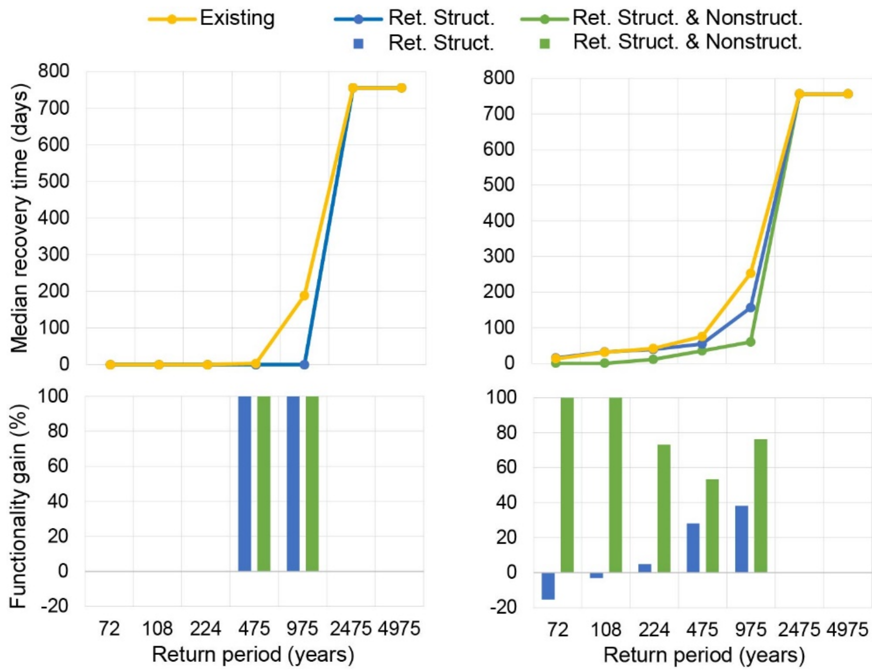

(a) (b)

Figure 3 and (a) (b)

Figure 4. The decline mainly occurred due to the retrofits' increase in the strength and stiffness of the buildings, which greatly improved the structural responses. For example, according to Figure S1, the SDR at the first story of W1 decreased by 55 % at the 475-year return period. As a

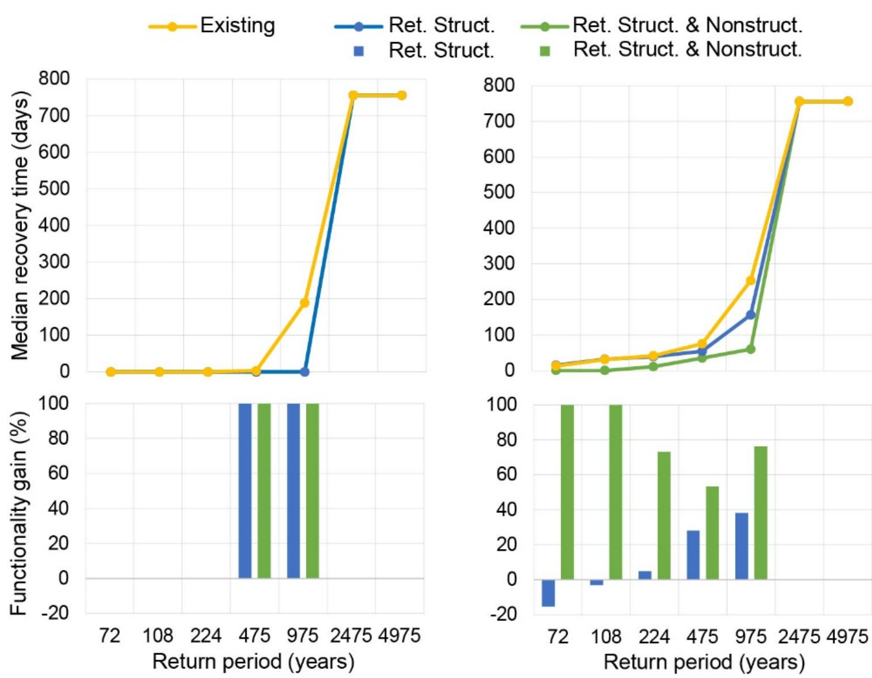

result,

(a) (b)

Figure 3 shows that the retrofit strategy that added wall boundary elements and increased wall thickness effectively improved the SDRs and reduced the recovery times by 100 % (from 3 days to 0 days) and 28 % (from 75 days to 54 days) for the reoccupancy and functional recovery performance states at the 475-year return period, respectively. Figure S5 shows that the SDR at the first story of F5 decreased by 75 % at the 224-year return period (for both building directions). At the 475-year return period, the existing building has a high (67%) probability of collapse and SDRs larger than 3 %, while SDR at the first story of the retrofitted building is around 0.6 % (in both directions). In consequence, in (a) (b)

Figure 4, the results for the structurally retrofitted model for this building indicate an improvement for the 475-year return period of 64 % (from 570 days to 207 days) and 59 % (from 570 days to 231 days) for the reoccupancy and functional recovery performance states, respectively. While W1 has the larger percent improvement for both performance states, F5 has the much larger improvement measured in number of days. Gains are also observable in lower hazard levels, confirming that the structural retrofit design substantially reduced recovery times for this building.

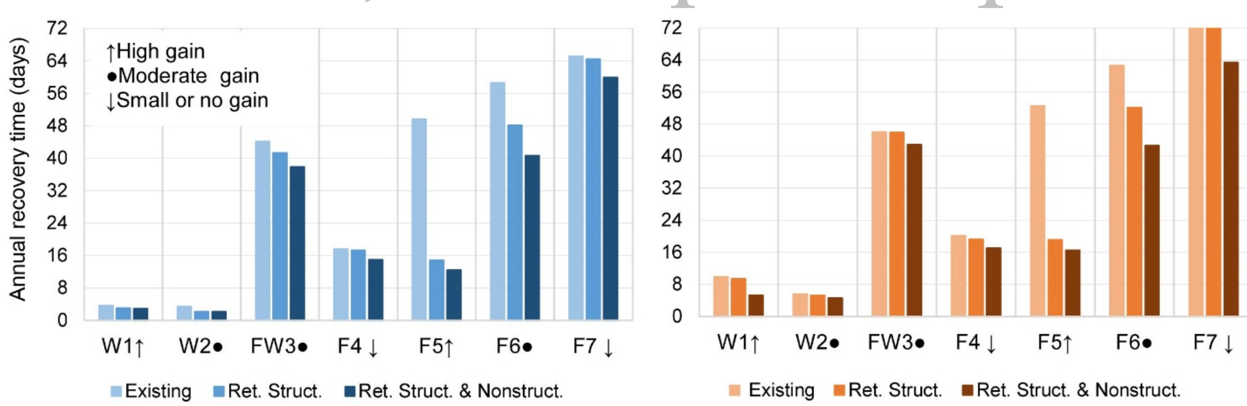

(a) (b)

Figure 2. Expected annual equivalent recovery times for (a) reoccupancy, and (b) functional recovery

These results, along with those in Table 3, show that the retrofit strategies applied to buildings W1 and F5 improved the collapse capacity of the existing buildings (2 % and 73 %, respectively) and their performance by reducing drift demands despite the increase in PFAs demands. As will be discussed in more detail later, these buildings' reoccupancy and function is driven in large part by drift-sensitive components, and the likelihood of this damage is reduced for the structurally retrofitted buildings. For example, as shown in Table S6, at the 475-year return period, all loss of reoccupancy and function is observed (i.e., 100 % of realizations affected) for the existing building F5, which reduced to about 80 % of realizations affecting reoccupancy and function for the structurally retrofitted building. However, as shown in Table S2, there is not a significant reduction in percent of realizations affecting function for W1, compared to the reduction for reoccupancy, because the structural retrofit strategies increased the PFAs and therefore the percent of acceleration-sensitive components affecting function remained high. This point is confirmed in

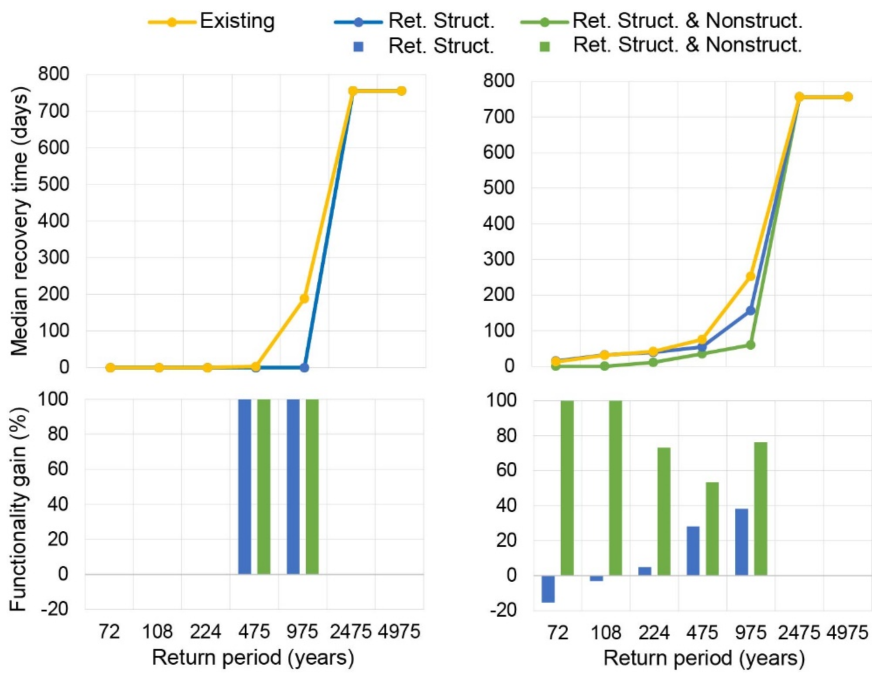

(a) (b)

Figure 3, where there is a greater gain for reoccupancy than for functional recovery through the structural retrofit at the 475-year return period. Due to the reduction of SDRs after retrofit, a reduction in the percent of realizations of displacement-sensitive systems affecting reoccupancy is observed, as reported in Table S2. However, due to the increase in PFA, Table S2 shows that the acceleration-sensitive components continue to affect the functional recovery time, which results in a greater improvement for reoccupancy compared to for functional recovery.

Buildings with moderate functionality gain

Buildings W2, FW3, and F6, had a moderate decrease in recovery times for reoccupancy and functional recovery performance levels. The structural retrofit of F6 involved adding a pair of viscous dampers to two spans of the first two stories and resulted in a moderate reduction in their recovery times. As shown in Figure S6, the SDR reduction is primarily visible in the first two stories. For example, a 11 % reduction of SDR at the first story resulted in moderate functionality gains of 8 % and 7 % for reoccupancy and functional recovery, respectively, at the 475-year return

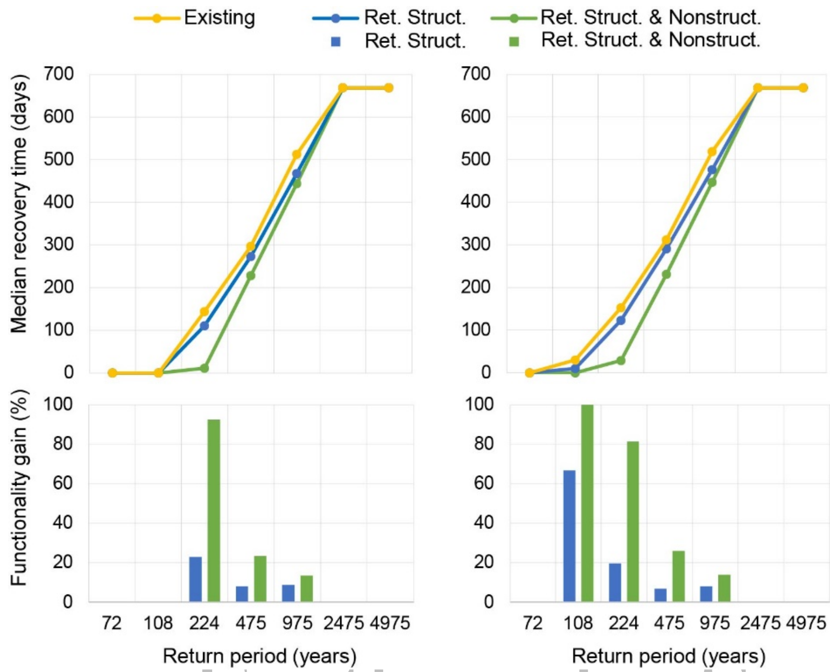

period (shown in

(a) (b)

Figure 5). Figure S6 also shows that adding viscous dampers can reduce the SDRs without significantly increasing floor accelerations, for example, less than 10 % increase in PFAs is observed at the 475-year return period. For this building, because the reduction of SDRs is not significant, the displacement-sensitive components continue affecting the reoccupancy and function of the building, and acceleration-sensitive components are not significantly reduced in their damage, such that neither the gain in reoccupancy nor functional recovery are significant.

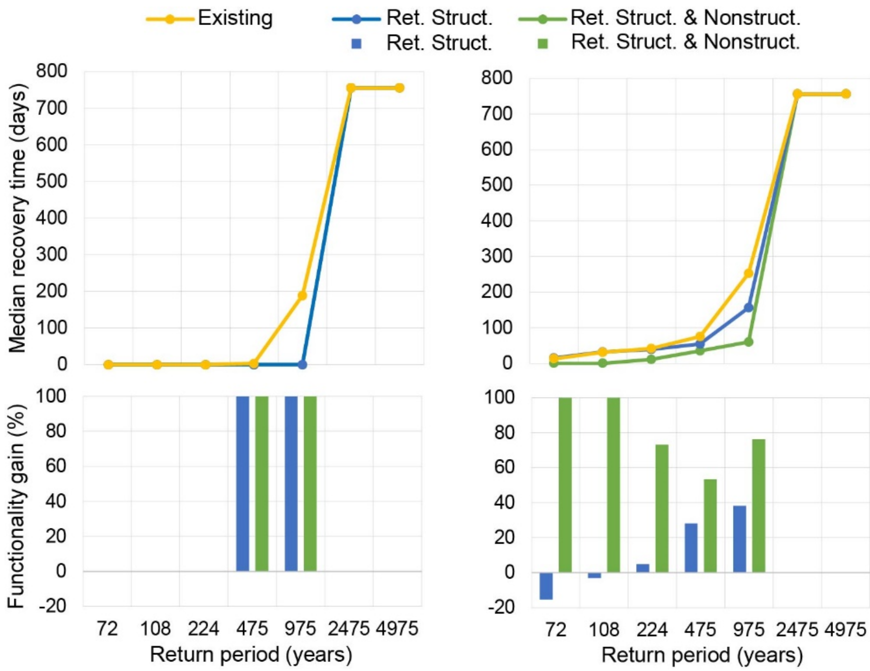

(a) (b)

Figure 3. Recovery times for W1, (a) Reoccupancy, and (b) Functional Recovery

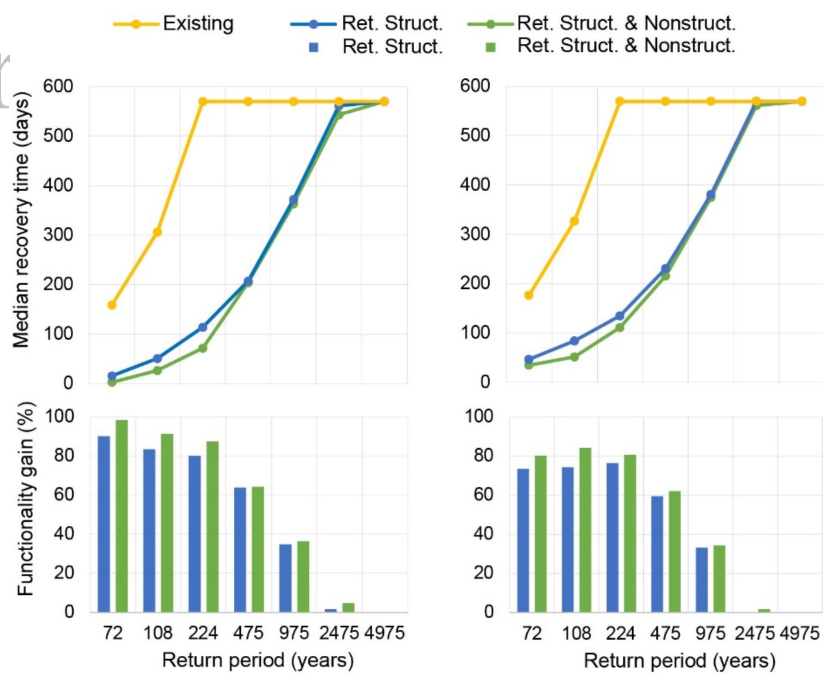

(a) (b)

Figure 4. Recovery times for F5, (a) Reoccupancy, and (b) Functional Recovery

The SDRs of W2, retrofitted by adding new transverse shear walls and FRPs at column ends of the existing transverse wall, show a moderate decline, according to Figure S2, also resulting in moderate functionality gains. In this case, the SDRs did not significantly improve through structural retrofit, and PFAs worsened somewhat, resulting in moderate gains for reoccupancy and functional recovery. For example, considering the 475-year return period in Figure S2, the SDR at the first story decreased by 22 % through the structural retrofit (45 % on average for all stories). However, due to the increase in stiffness and reduction in inelastic action of W2 (also shown in Figure S2), PFAs moderately increased by 18 % on average in both building´s directions. As a result, according to Figure S8, we see 38 % and 24 % functionality gains for reoccupancy and functional recovery performance states, respectively, at the 475- year return period.

Similarly, building FW3, which was retrofitted by strengthening the perimeter perforated walls with piers and spandrels, as well as strengthening the perimeter column foundations, showed an average decrease in SDR by 34% and an average increase in PFAs by 28 % for the 475-year return period by the structural retrofit (see Figure S3). This resulted in 18 % functionality gain for both reoccupancy and functional recovery performance states. (Figure S9). The overall structural performance of this building was moderately improved through retrofit, considering that the owner desired to preserve the historic character of the building while complying with the design code requirements. Therefore, moderate improvements resulted in moderate functionality gains.

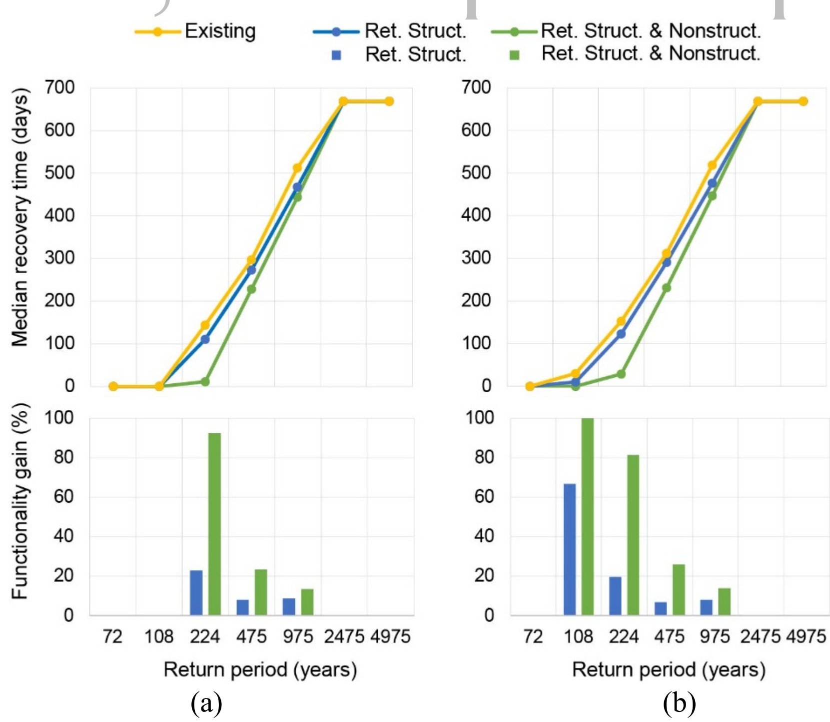

Figure 5. Recovery times for F6, (a) Reoccupancy, and (b) Functional Recovery

Buildings with low functionality gain

Buildings F4 and F7 showed the lowest functionality gains among the buildings because the retrofit strategy for these buildings was minor and less impactful on the seismic responses compared to other designs. F7's structural retrofit was minor and localized (mainly focused on the first two stories). The building was occupied during the retrofit, and the owner desired to preserve the historic properties of the building while performing voluntary seismic improvements. Thus, the minor structural stiffening enhancements resulted in a decrease of 19 % on average of the SDR at the first story in both directions at the 224 -year return period (Figure S7). Therefore, we estimated about 5 % gains for both reoccupancy and functional recovery performance states at this

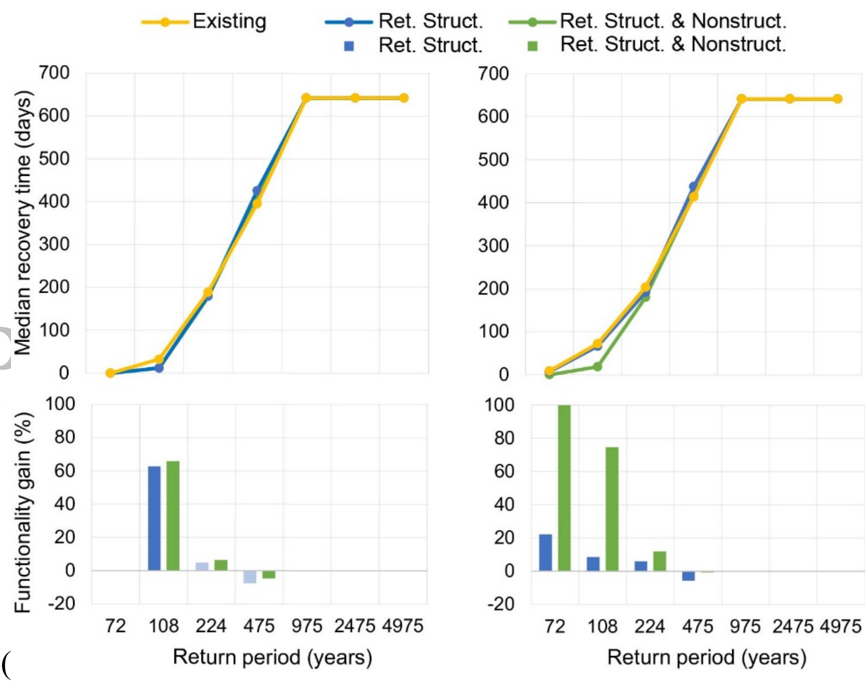

hazard level (

(a) (b)

Figure 6). However, the adopted retrofit strategy did not help for the 475-year return period and resulted in about 8 % and 6 % increase in time for reoccupancy and functional recovery states, respectively. This retrofit actually resulted in a minor increase in drifts for this hazard level (about 13 %, according to Figure S7). We hypothesize that this worse performance occurs because the unsymmetric retrofit solutions increased torsion and did not fundamentally improve deformation capacity (hence, the 475-year return period is worse than the 224- year return period).

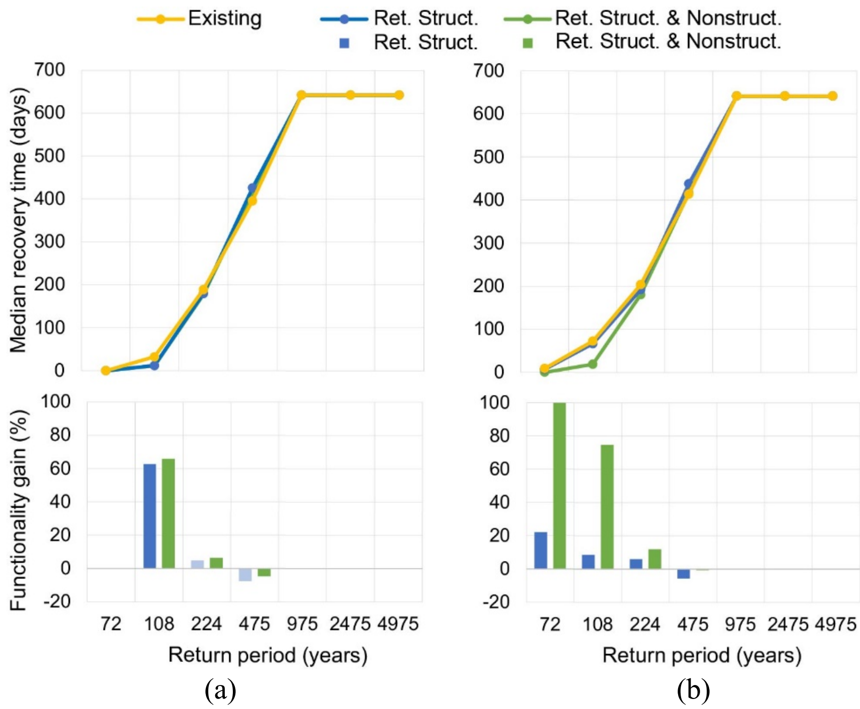

Figure 6. Recovery times for F7, (a) Reoccupancy, and (b) Functional Recovery

Table S8 show a high percent of realizations of displacement-sensitive systems affecting building reoccupancy and function, and because the structural retrofit strategies did not help to reduce the SDRs or avoid red tags, it is not possible to see significant functionality gains for either performance level. Similarly, for F4, the retrofit involved addition of a small number of slender walls, which did not significantly affect the EDPs and therefore the performance.

Effect of nonstructural retrofit

This section discusses the efficacy of nonstructural retrofit strategies applied in addition to the structural retrofits. Generally, buildings having high functionality gains with the structural retrofit typically also present relatively high functionality gains with the structural and nonstructural retrofit (e.g., W1 and F5). This occurs because EDP levels are strongly related to structural and nonstructural damage. Nevertheless, the impact of structural retrofit on EDPs, both SDRs and PFAs, influences which nonstructural systems most need to be retrofit. For example, the structural retrofit strategies that consist of adding shear walls in some cases dramatically increase stiffness. In that case, a decrease in SDRs and an increase in PFAs is generally observed. Thus, retrofitting the acceleration sensitive nonstructural components may be needed because the damage to these components could cause the building's functional recovery time to increase.

In general, we identified two groups: (1) buildings in which reoccupancy is dominated by components sensitive to displacement and function by components sensitive to acceleration (W1, F5), and (2) buildings in which both reoccupancy and function are dominated by displacement-sensitive components, but function is also affected by acceleration-sensitive components (W2, FW3, F4, F6 and F7). The effect of nonstructural retrofit is different for the two groups.

For the first group, the function gain came from reducing reoccupancy problems. For example, for building W1, reoccupancy is affected by displacement-sensitive components and systems, especially damaged structural components contributing to a red tag. From structural retrofit, reoccupancy times reduced by decreasing drifts, which in turn improves function. After retrofit, primarily acceleration-sensitive components (e.g., HVAC systems) are affecting function (see Table S2). For W1 (see Figure S1), the retrofit strategy resulted in an increase in PFAs of approximately 10% at all the floors for the 475-year return period. When the nonstructural retrofit is also considered, the acceleration-sensitive HVAC components trigger function problems less often (see Table S2, reducing the realizations that trigger function problem in these systems from 60% to 40% at the 475-year return period).

On the contrary, for group 2, for example, for building F6 in Table S7, displacement-sensitive systems affecting the existing's building reoccupancy (e.g., problems with stairs and entry doors). The structural retrofit did not significantly change the drift demands, producing about 8 % gains for reoccupancy and functional recovery performance levels at the 475-year return period. As a result, the displacement-sensitive systems continue to affect not only reoccupancy, but also function. As a result, in this case, the retrofit of displacement-sensitive systems was essential in the nonstructural upgrades. For the existing and structurally retrofit buildings (Table S7), displacement-sensitive stairs triggered the highest percentage of realizations at the 475-year return period. The retrofit of the stairs in the nonstructural upgrades produced the further improvement of about 15% in reoccupancy and recovery times.

Important hazard levels

Among the results presented so far, we have focused on the EAT (which combines all hazard levels) and results at the 475-year return period. Yet, identifying the hazard levels that matter for achieving recovery-based objectives through a resilient retrofit design is critical for decision-

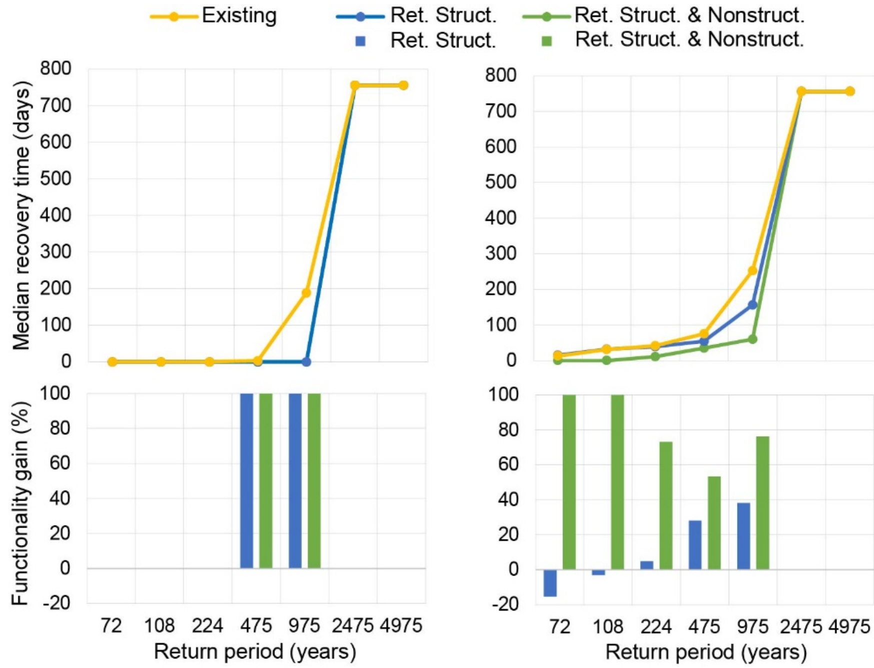

making. As

(a) (b)

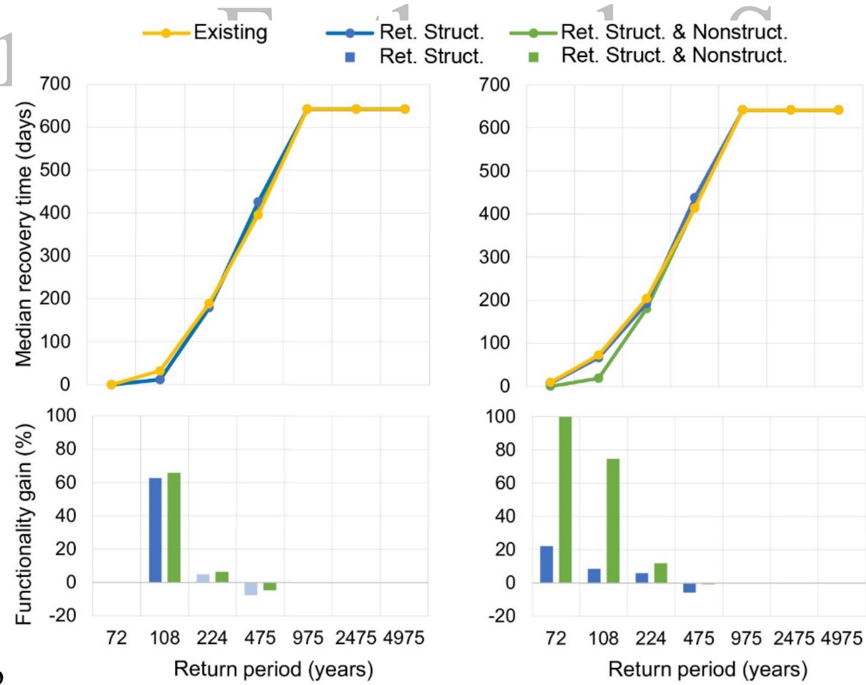

Figure 3 to

(a) (b)

Figure 6 show, the general trend is that at lower hazard levels, the retrofit does not significantly affect the recovery goals. In the middle hazard levels, we see the largest benefit. Finally, at the highest hazard levels there is not much benefit.

Consider, for example, the highest shaking levels. In these cases, both the existing and structural retrofit buildings perform relatively poorly with high collapse risk, and there is no benefit from the retrofit. These hazard levels correspond to those that exceed the median collapse capacity of both the existing and retrofitted cases. For W1, for example, this occurs at about the 2475-year return period (

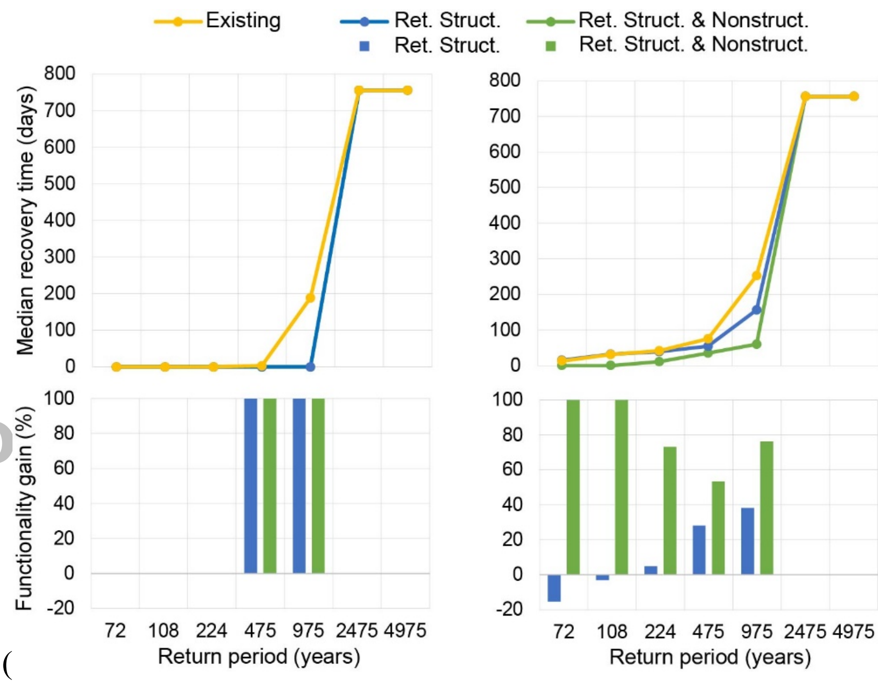

(a) (b)

Figure 3). Higher collapse capacities achieved in retrofit, therefore, widen the range of hazard levels at which functional recovery benefits can be obtained.

At the lowest shaking levels, again, most of the retrofit designs of buildings did not significantly improve the recovery times. At the lowest levels, there is no damage to structural and nonstructural components that delay buildings' recovery, therefore retrofit to improve recovery time for frequent earthquakes may not be needed. Indeed, in two cases, FW3 and F4, the results show a functionality loss (negative functionality gain) at the 72 and 108-year return periods for functional recovery. After minor structural upgrades to the FW3 building, SDRs not only do not decrease, but increase by up to 53 %, and PFAs also increase.

The intermediate intensity measures are those in which the benefits of improved structural performance are most apparent. For example, for building W1, the highest functionality gains for reoccupancy and functional recovery performance levels occurred at the 475 and 975-year return

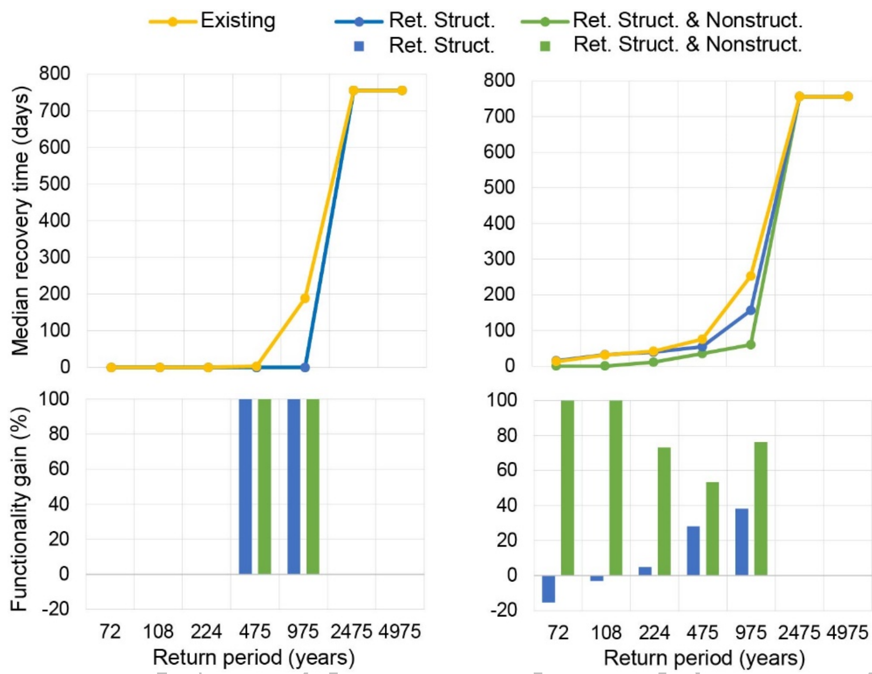

periods, as shown in

(a) (b)

Figure 3. This result is associated with the reduction by up to 55 % in SDRs at these hazard levels compared to the maximum reduction in SDRs of 40 % observed at lower hazard levels. A reader might suggest that these SDR changes are not so far apart as to make a significant difference in functionality gains. However, due to the brittle behavior of this building, discussed in detail in Echeverria et al. (2022), a slight improvement in demands may be critical for achieving functional recovery goals.

FUNCTIONAL RECOVERY IN RELATION TO OTHER PERFORMANCE GOALS

Economic Losses

Functional recovery objectives are relatively new to the earthquake engineering profession. As a result, we consider whether a more familiar metric may provide meaningful correlation to functional recovery assessment. Figure 7 compares economic losses in terms of EALs to EAT for the different buildings.

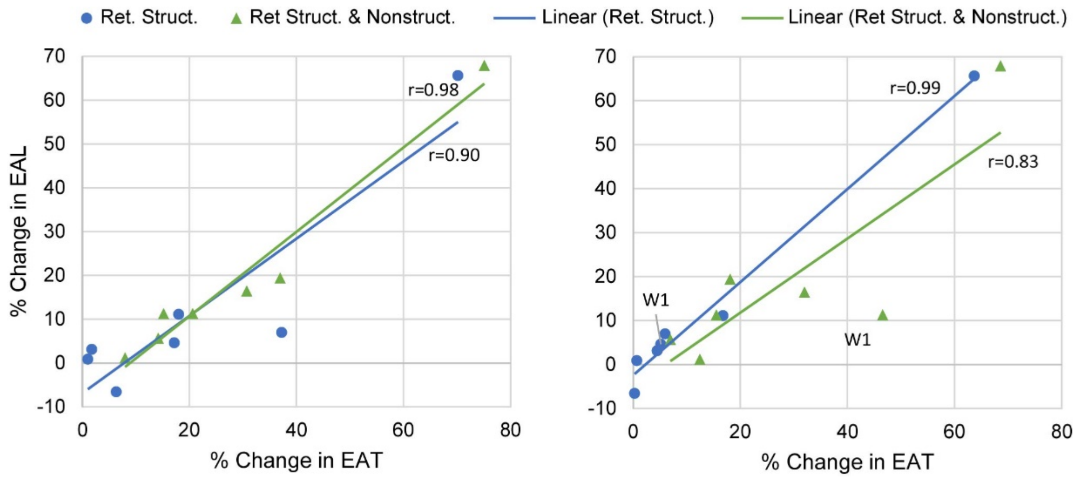

(a) (b)

Figure 7. Percent change in EAL vs in EAT of buildings with structural and structural and nonstructural retrofit with respect to the existing buildings for (a) reoccupancy, and (b) functional recovery

In general, we see strong linear trend and high correlation (r = 0.9 to 0.98) between the percent change in EAL and in EAT for reoccupancy when structural retrofit and structural together with nonstructural retrofit are implemented. For the functional recovery performance state, stronger linear correlation (r = 0.99) is observed when structural retrofit is adopted as well. However, this relationship between the variables is less strong (r = 0.83) for the case in which structural together with nonstructural retrofit is considered. For example, as displayed in Figure 7(b), for the structural retrofit of the W1 building (the annotated blue point), a low to moderate change in EAL corresponds to a low percent change in EAT. On the contrary, when nonstructural retrofit is included for this building (the annotated green point), a higher percent change in EAT is possible, even when the change in EAL remains low. This discrepancy occurs because systems that correspond to high repair costs do not correspond to high loss of function and vice versa, and greater benefits in time are achieved because the retrofits target those nonstructural components that most affect function. The structural retrofits inherently address items with high repair costs that drive reoccupancy metrics.

ASCE 41's Immediate Occupancy Limits

ASCE/SEI 41 expresses concepts similar to functional recovery in its definition of IO. Acceptance criteria for IO are based on structural component deformations. To explore the relation between the IO performance in ASCE/SEI 41 and the functional recovery assessment, we focus on building W1, whose performance is governed by a single component, the flag-shaped RC wall.

Table 10-19 of ASCE/SEI 41 shows that the thresholds in terms of plastic hinge rotations for wall components responding in flexure like the walls of W1 are 0.001 and 0.0015 for IO for the existing and retrofitted buildings, respectively (ASCE/SEI, 2017). Figure 8 compares the median recovery times for reoccupancy and functional recovery performance states of W1 with the probability of exceeding the IO limit states defined in ASCE 41. The exceedance probability is calculated as the fraction of ground motions at each stripe level for which the hinge rotations of the wall element in W1 exceed the corresponding limit state.

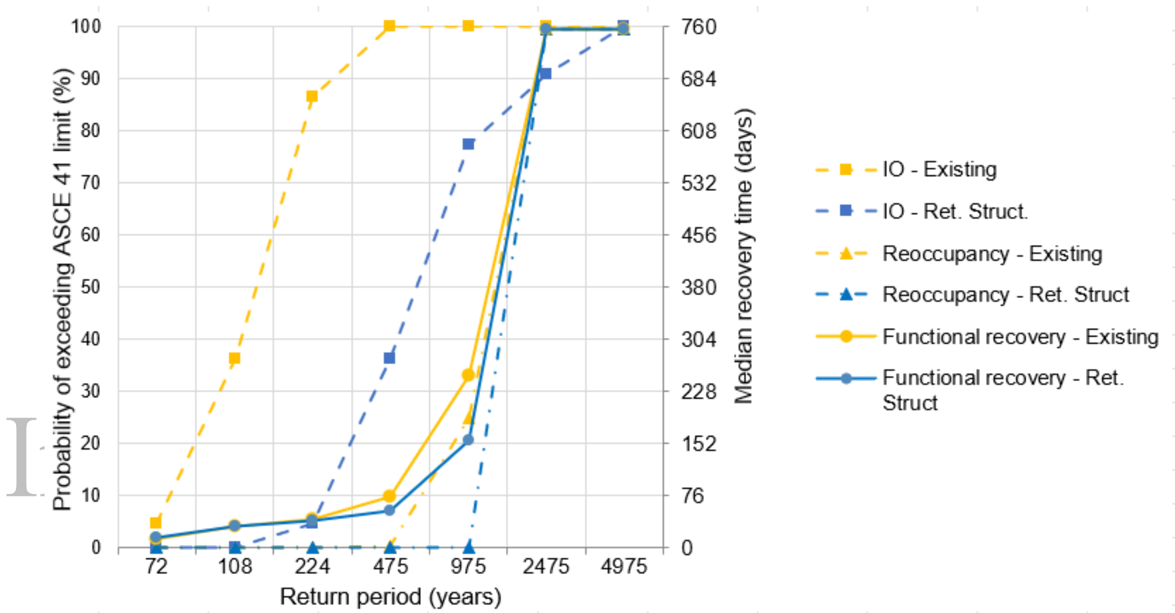

Figure 8. Comparison of recovery times with the probability that the ASCE 41's IO limit state is exceeded for W1

For the existing building, these results suggest that the chance of exceeding the IO limit greatly increases after the 72-year return period. However, the reoccupancy and functional recovery times increase at higher intensities (return periods). For the structurally retrofitted building, a similar trend is visible, though the probability of exceeding the IO limit increases at more similar intensities to the significant increase in recovery than in the existing building. These observations, for only one building, suggest that the IO limits may be conservative as a metric of functional recovery, meaning IO fails before functional recovery drastically increases. This trend is likely due to the use of component (structural) limits that reflect primarily the worst offending structural component. We also observe less of a performance "cliff" of functional recovery and reoccupancy as a function of intensity.

CONCLUSIONS

This paper explores the feasibility of improving post-earthquake recovery times through seismic retrofit. Seven existing reinforced concrete buildings with a variety of lateral load-resisting systems are explored, and their results from the seismic performance and functional recovery assessments are compared with those obtained for their corresponding retrofitted cases. Two retrofit cases are considered for each building: (1) retrofit of structural components, and (2) retrofit of structural and nonstructural components. The structural upgrades include adding new walls, dampers, and fiber reinforced polymers, while the nonstructural retrofit strategies mainly involve adding seismic joints to stairs, improving elevators, replacing conventional systems with certified systems, and adding seismic anchors to the equipment.

As expected from the life safety focus of many of the retrofits, retrofit often has a significant influence on collapse capacity. For the buildings (W1 to F5) with major structural upgrades, such as the addition of new shear walls, which increase the global building stiffness, results show greater improvements in the collapse capacity, a decrease in drifts and an increase in floor accelerations. For the other buildings, the effects on collapse capacity are more modest, with mixed or moderate effects on other engineering demands. For the building (F6) retrofitted using dampers, results reflect a moderate reduction in lateral drifts after installation of the dampers, without a significant increase in accelerations. For a building (F7) with minor or local structural upgrades, including strengthening of transfer beams and diaphragm connections, a slight decrease in drifts and an increase in floor accelerations is observed.

The functional recovery assessment, in terms of expected annual recovery times, shows that the structural retrofit of buildings generally reduces these EATs. The effect of the structural retrofit on EAT depends on the building and the structural retrofit strategy, ranging from less than a 1 % (F7) to about 70 % reduction (F5) for the reoccupancy and functional recovery performance levels. Incorporating the retrofit of nonstructural components can provide additional reduction in EATs, mainly for functional recovery performance level.

These results allow us to classify three groups of buildings: (1) high, (2) moderate, and (3) small functionality gains. First, the effect of structural retrofit is examined. The results reveal that among the buildings with high functionality gain are those in which there is a substantial improvement in the seismic performance and collapse capacity through structural retrofit, mainly those buildings (W1, F5) in which the increase in strength and stiffness led to a considerable reduction in story drifts. The reduction in drifts lead to a significant decrease in the recovery times, even when there is an increase in acceleration demands after the structural retrofit. In group (2) are those buildings in which a moderate reduction in drifts is achieved with the structural retrofit, resulting in a moderate increase in functionality gains. For example, for the building (F6) retrofitted by adding viscous dampers, a moderate reduction in drifts occurs in the retrofit stories without significantly increasing floor accelerations, resulting in a moderate functionality gain for the two performance levels. Finally, in the third group are those buildings in which a small, zero or even negative functionality gain is observed, mainly where minor or local structural retrofit slightly affect the EDPs and do not significantly improve global collapse performance (F7).

Considering the combined structural and nonstructural retrofits, results also reveal that where structural retrofits reduce drifts but significantly increase floor accelerations (W1), the retrofit of acceleration-sensitive nonstructural components is needed to further improve the functional recovery time. On the other hand, where structural retrofits moderately or slightly reduce drifts (F6), the displacement-sensitive nonstructural components continue to affect reoccupancy and function after retrofit. In these cases, the retrofit of nonstructural components may not considerably improve recovery times because many of which are acceleration-sensitive components, and because some of the structural issues (i.e., red tags) are not appreciably reduced.

This study also explores the hazard level or levels in which the retrofit strategies may be most effective in improving recovery times. The results show that seismic retrofit is most effective for intermediate hazard levels, showing the highest functionality gains, but is not effective at lower levels and at the highest levels of hazard. This can be explained because, at lower levels, some of the retrofit designs of buildings not only do not help improve the demands but could make them worse, and at the highest hazard level existing and retrofitted buildings may reach collapse; therefore, there is no benefit from the retrofit.

Finally, results from functional recovery assessment are related to other more familiar metrics or performance goals. First, we compare our results to those expressed in losses (repair costs). In general, and especially in the case of structural retrofit only, there is a strong linear correlation is observed between percent changes in EATs and percent changes in EALs, i.e., systems that correspond to high repair cost correspond to high loss of function. However, in some cases, especially considering the metric of functional recovery time, the systems that have highest repair costs do not have the highest impact on function, which could produce mistaken recommendations if losses were used as a proxy for function. Then, we also compare the functional recovery results with the immediate occupancy limit defined in the seismic retrofit and evaluation standard, ASCE/SEI 41. We conclude that the IO limits may be a conservative metric compared to functional recovery due to being focused on critical components' performance.

The findings of this study are critical for engineers and policymakers to evaluate the feasibility of achieving functional recovery goals through the seismic retrofit of existing buildings. It shows that functional recovery improvements may be possible alongside life safety retrofits, particularly if both drifts and accelerations are controlled through the retrofit. Building standards or guidelines to facilitate design and assignment to meet these goals are needed.

ACKNOWLEDGMENTS

Financial support for this work was provided by the U.S. Department of Commerce, National Institute of Standards and Technology under the Financial Assistance Award Number #70NANB19H058. This financial support is gratefully acknowledged. The views expressed are those of the authors and may not represent the official position of the National Institute of Standards and Technology or the U.S. Department of Commerce. We also gratefully acknowledge the engineers who provided information about building drawings and retrofit designs and Mr. Ed Almeter and Dr. Curt Haselton for facilitating the use of the SP3 software. Certain commercial software may have been used in the preparation of information contributing to this paper. Identification in this paper is not intended to imply recommendation or endorsement by NIST, nor is it intended to imply that such software is necessarily the best available for the purpose.

REFERENCES

Abdullah SA and Wallace JW (2021) Drift capacity at axial failure of RC structural walls and wall piers. *Journal of Structural Engineering* 147(6): 04021062.

Aghababaei M, Okamoto C and Koliou M (2022) Examining the accuracy and validity of loss estimations using the PBEE methodology for wood residential buildings through integrated experimental findings and expert panel solicitation. *Sustainable and Resilient Infrastructure* 7(5): 638-654.

Alesch D, Holly J and Nagy R (1998) Small business failure, survival and recovery: lessons from the January 1994 Northridge Earthquake. *NEHRP Conference and Workshop on Research on the Northridge, California Earthquake of January.* 1994.

Almufti I and Willford M (2013) REDi™ rating system: Resilience-based earthquake design initiative for the next generation of buildings. *Arup Co* https://www.arup.com/perspectives/publications/research/section/redi-rating-system.

ASCE/SEI (2016) *Minimum Design Loads and Associated Criteria for Buildings and Other Structures.* American Society of Civil Engineers.

ASCE/SEI (2017) *Seismic Evaluation and Retrofit of Existing Buildings* American Society of Civil Engineers.

ATC (2021) (ATC 138-3) Seismic Performance Assessment of Buildings, Volume 8 – Methodology for Assessment of Functional Recovery Time In: *Federal Emergency Management Agency*, Washington, D.C. .

Baker JW (2015) Efficient analytical fragility function fitting using dynamic structural analysis. *Earthquake Spectra* 31(1): 579-599.

Bonowitz D (2011) Resilience criteria for seismic evaluation of existing buildings: a 2008 special projects initiative report to structural engineers association of northern california. Report. *Structural Engineers Association of Northern California (SEAONC)*.

Buckalew J, Bonowitz D, Mayes R, et al. (2020) Understanding Community Resilience and Functional Recovery; By the SEAOC Resilience Committee. *Structural Engineers Association of California (SEAOC) Newsletter*.

California Legislature (2021) *Assembly Bill (AB)-1329*. Available at: https://leginfo.legislature.ca.gov/faces/billNavClient.xhtml?bill_id=202120220AB1329 (accessed October 4, 2022).

Cimellaro GP and Piqué M (2016) Resilience of a hospital emergency department under seismic event. *Advances in Structural Engineering* 19(5): 825-836.

Collins B (1995) Chatsworth : Post Office Repaired, Set to Reopen Sept. 5. *Los Angeles Times*.

Cook D, Fitzgerald K, Chrupalo T, et al. (2017) Comparison of FEMA P-58 with other building seismic risk assessment methods. *Chico, California, available at: http://static-assets. hbrisk. com/reports/RiskAssessmentComparisonReport_FEMA-P-58-to-OtherMethods_2017_03_08. pdf.*

Cook D and Sattar S (2022a) The Effect of Increased Strength and Stiffness Requirements on the Functional Recovery Performance of Reinforced Concrete Special Moment Frames. In: *12th National Conference on Earthquake Engineering (12NCEE)*, Salt Lake City, UT.

Cook D and Sattar S (2022b) The Impact of Nonstructural Damage on Building Function. In: *Fifth International Workshop on the Seismic Performance of Non-Structural Elements (SPONSE)*, Palo Alto, CA.

Cook DT (2021) *Advancing Performance-Based Earthquake Engineering for Modern Resilience Objectives*. University of Colorado at Boulder.

Cook DT and Liel AB (2021) Component response metrics for indication of global collapse. *Bulletin of Earthquake Engineering* 19(15): 6469-6496.
Cook DT, Liel AB, Haselton CB, et al. (2022) A framework for operationalizing the assessment of post-earthquake functional recovery of buildings. *Earthquake Spectra*. 87552930221081538.
Dabaghi M, Saad G and Allhassania N (2019) Seismic collapse fragility analysis of reinforced concrete shear wall buildings. *Earthquake Spectra* 35(1): 383-404.
Davidson RA, Kendra J, Ewing B, et al. (2022) Managing disaster risk associated with critical infrastructure systems: a system-level conceptual framework for research and policy guidance. *Civil Engineering and Environmental Systems*. 1-21.
Deierlein GG, Reinhorn AM and Willford MR (2010) Nonlinear structural analysis for seismic design. *NEHRP seismic design technical brief* 4: 1-36.
Echeverria MJ, Jünemann R and Liel AB (2022) Seismic fragility assessment of medium-rise fishbone-type reinforced concrete wall buildings. *Journal of Building Engineering* 59: 105044.
Echeverria MJ, Mohammadgholibeyki N, Liel AB, et al. (2023) Achieving Functional Recovery through Seismic Retrofit of Existing Buildings: Barriers and Opportunities. *Performance of Constructed Facilities* Forthcoming.
EERI (2019) Functional Recovery: A Conceptual Framework. *White Paper*.
Egbelakin T, Wilkinson S and Ingham J (2014) Economic impediments to successful seismic retrofitting decisions. *Structural Survey* 32(5): 449-466.
Feenstra PH (1993) Computational aspects of biaxial stress in plain and reinforced concrete. *PhD thesis, Delft Univ. of Technology*.
FEMA (2009) Quantification of building seismic performance factors. In: *Federal Emergency Management Agency*, Washington DC.
FEMA (2012) Seismic performance assessment of buildings, Implementation Guide. In: *Federal Emergency Management Agency*, California.
FEMA (2013) Multi-hazard loss estimation methodology, earthquake model, HAZUS-MH 2.1 Technical Manual. In: *Federal Emergency Management Agency*, Washington DC, pp.699.
FEMA (2018) Seismic Performance Assessment of Buildings: Volume 1- Methodology In: *Federal Emergency Management Agency*, Washington, DC.
Filippou F, Popov E and Bertero V (1983) *Effects of Bond Deterioration on Hysteretic Behavior of Reinforced Concrete Joints.* Berkeley, California: Earthquake Engineering Research Center University of California; For sale by the National Technical Information Service U.S. Dept. of Commerce.
Harrington CC and Liel AB (2020) Evaluation of seismic performance of reinforced concrete frame buildings with retrofitted columns. *Journal of Structural Engineering* 146(11): 04020237.
Haselton Baker Risk Group (2022) *Seismic Performance Prediction Program (SP3)*. Available at: www.hbrisk.com (accessed 12.06.2022).
Haselton C, Almeter E, DeBock D, et al. (2020) Legislative Efforts in the United States to Change Building Code Requirements from Safety-Only-Based Design to Functionality-Based (Resilient) Design. In: *17th World Conference on Earthquake Engineering*, Sendai, Japan.
HCAI (2022) *HCAI Special Seismic Certification Preapproval (OSP)*. Available at:

https://hcai.ca.gov/construction-finance/preapproval-programs/oshpd-special-seismic-certification-preapproval-osp/ (accessed November 12, 2022).
Hordijk D and Reinhardt H (1993) Numerical and experimental investigation into the fatigue behavior of plain concrete. *Experimental mechanics* 33(4): 278-285.
Ibarra LF, Medina RA and Krawinkler H (2005) Hysteretic models that incorporate strength and stiffness deterioration. *Earthquake Engineering & Structural Dynamics* 34(12): 1489-1511.
Jacques CC, McIntosh J, Giovinazzi S, et al. (2014) Resilience of the Canterbury hospital system to the 2011 Christchurch earthquake. *Earthquake Spectra* 30(1): 533-554.
Jalayer F and Cornell C (2009) Alternative non-linear demand estimation methods for probability-based seismic assessments. *Earthquake Engineering & Structural Dynamics* 38(8): 951-972.
Kent DC and Park R (1971) Inelastic behaviour of reinforced concrete members with cyclic loading. *Bulletin of the New Zealand Society for Earthquake Engineering* 4(1): 108-125.
Kim JJ, Elwood KJ, Marquis F, et al. (2017) Factors influencing post-earthquake decisions on buildings in Christchurch, New Zealand. *Earthquake Spectra* 33(2): 623-640.
Kourehpaz P, Molina Hutt C, Marafi NA, et al. (2021) Estimating economic losses of midrise reinforced concrete shear wall buildings in sedimentary basins by combining empirical and simulated seismic hazard characterizations. *Earthquake Engineering & Structural Dynamics* 50(1): 26-42.
Li L, Chang-Richards A, Boston M, et al. (2022) Seismic resilience vs. Functional recovery of buildings: A critical review. In: *NewZealand Society for Earthquake Engineering 2022 NZSEE conference*, Online.

Menegotto M (1973) Method of analysis for cyclically loaded RC plane frames including changes in geometry and non-elastic behavior of elements under combined normal force and bending. *Proc. of IABSE symposium on resistance and ultimate deformability of structures acted on by well defined repeated loads.* 15-22.
Miano A, Sezen H, Jalayer F, et al. (2019) Performance-based assessment methodology for retrofit of buildings. *Journal of Structural Engineering* 145(12): 04019144.
Mitrani-Reiser J (2007) *An ounce of prevention: probabilistic loss estimation for performance-based earthquake engineering*. California Institute of Technology.
Miyamoto K, Gilani AS and Determan L (2017) Seismic Retrofit And FEMA P-58 Risk Assessment Of Mid-Rise Soft-Story Concrete Towers. *Taylor Devices Inc.*
Molina Hutt C (2022) *TREADS: Tool for Recovery Estimation And Downtime Simulation of buildings*. Available at: https://github.com/carlosmolinahutt/treads (accessed May 1, 2023).
Molina Hutt C, Hulsey AM, Kakoty P, et al. (2022a) Toward functional recovery performance in the seismic design of modern tall buildings. *Earthquake Spectra* 38(1): 283-309.
Molina Hutt C, Vahanvaty T and Kourehpaz P (2022b) An analytical framework to assess earthquake-induced downtime and model recovery of buildings. *Earthquake Spectra* 38(2): 1283-1320.
NIST (2022) Benchmarking Evaluation Methodologies for Existing Reinforced Concrete Buildings. In: *National Institute of Standards and Technology*, Gaithersburg, MD.
NIST/FEMA (2021) NIST-FEMA Special Publication FEMA P-2090/NIST SP-1254: Recommended options for improving the built environment for post-earthquake reoccupancy and functional recovery time. In: *National Institute of Standards and*

Technology Gaithersburg, MD.
Paul N, Almufti I, Mieler M, et al. (2018) Estimation of post-earthquake recovery on a university campus using REDi methodology. *Proceedings of the 11th US National Conference on Earthquake Engineering, Los Angeles, California.*
PEER (2005) Van Nuys hotel building testbed report: exercising seismic performance assessment. In: *Pacific Earthquake Engineering Research Center, College of Engineering* Berkeley, CA.
Porter KA (2016) Safe enough? A building code to protect our cities and our lives. *Earthquake Spectra* 32(2): 677-695.
Rodgers J, Hassan W, Motter C, et al. (2021) Impacts of the 2018 M7. 1 Anchorage earthquake on schools. *Earthquake Spectra* 37(3): 1849-1874.
SEAOSC (2016) *Safer Cities Survey*. Available at: https://www.seaosc.org/resources/Summit/2016SaferCitiesSurvey.pdf (accessed September 20, 2020).
Stevenson JR, Kachali H, Whitman Z, et al. (2011) Preliminary observations of the impacts the 22 February Christchurch earthquake had on organisations and the economy: a report from the field (22 February–22 March 2011). *Bulletin of the New Zealand Society for Earthquake Engineering* 44(2): 65-76.
Taghvaei P (2022) *Evaluating the functional recovery performance of modern residential tall reinforced concrete shear wall buildings in Metro Vancouver*. University of British Columbia.
TBI (2017) Guidelines for performance-based seismic design of tall buildings. In: *Pacific Earthquake Engineering Research Center, College of Engineering* Berkeley, CA.
Terzic V and Kolozvari K (2022) Probabilistic evaluation of post-earthquake functional recovery for a tall RC core wall building using F-Rec framework. *Engineering Structures* 253: 113785.
Terzic V and Villanueva PK (2021) Method for probabilistic evaluation of post-earthquake functionality of building systems. *Engineering Structures* 241: 112370.
Terzic V, Villanueva PK, Saldana D, et al. (2021) Framework for modelling post-earthquake functional recovery of buildings. *Engineering Structures* 246: 113074.
WBDG (2016) *Precast Concrete Wall Systems*. Available at: https://www.wbdg.org/guides-specifications/building-envelope-design-guide/wall-systems/precast-concrete-wall-systems (accessed November 12, 2022).
Yavari S, Chang SE and Elwood KJ (2010) Modeling post-earthquake functionality of regional health care facilities. *Earthquake Spectra* 26(3): 869-892.
Zhan S, Chang-Richards A, Elwood K, et al. (2022) Post-earthquake functional recovery: A critical review. In: *NewZealand Society for Earthquake Engineering 2022 NZSEE conference*, Online.
Zhang Y, Fung JF, Johnson KJ, et al. (2022) Motivators and impediments to seismic retrofit implementation for wood-frame soft-story buildings: A case study in California. *Earthquake Spectra* 38(4): 2788-2812.